Ukrainian Journal of Physical Optics
ISSUE 1
2024

TEMPERATURE DEPENDENCES OF REFRACTIVE INDICES AND OPTICAL BIREFRINGENCE IN AMMONIUM FLUOROBERYLLATE

B. I. HORON [1,2 *], O. S. KUSHNIR [2] AND V. YO. STADNYK [1]

[1] Department of General Physics, Ivan Franko National University of Lviv, 19 Drahomanov Street, 79005 Lviv, Ukraine
[2] Optoelectronics and Information Technologies Department, Ivan Franko National University of Lviv, 107 Tarnavskyi Street, 79017 Lviv, Ukraine
[*] bohdan.horon@lnu.edu.ua

Received: 23.08.2023

Abstract. Refractive indices and optical birefringence of improper ferroelectric ammonium fluoroberyllate (AFB) crystals with the incommensurate phase are studied in a wide temperature range. Temperature characteristics of the optical indicatrix of AFB are examined and two quasi-isotropic points are found, the temperature positions T_0 of which are almost independent of the light wavelength. Unlike the dielectric permittivity affected by the incommensurate–ferroelectric phase transition (PT) at T_C, the optical characteristics of AFB are influenced only by the normal–incommensurate PT located at $T_i \approx 183.1$ K. Using a Ginzburg criterion and the experimental Ginzburg number $G \approx 2.5 \times 10^{-3}$, we have determined the temperature region around T_i where the critical fluctuations are small and a canonical mean-field theory can be applied. Outside the critical region, the spontaneous birefringence arising due to the incommensurate PT is described perfectly by the Landau theory, with the critical index of the order parameter $\beta \approx 0.50$.

Keywords: ammonium fluoroberyllate, optically biaxial crystals, refractive indices, optical birefringence, quasi-isotropic states, normal–incommensurate phase transitions, Ginzburg criterion, critical indices.

UDC: 535.323, 535.5, 535.012, 548.0, 536.77
DOI: 10.3116/16091833/Ukr.J.Phys.Opt.2024.01020;

1. Introduction

Ammonium fluoroberyllate $(NH_4)_2BeF_4$ abbreviated hereafter as AFB is one of canonical ferroelectric crystals attracting much attention of researchers [1–5]. Like in some of A_2BX_4 compounds, the normal phase in AFB above $T_i \approx 183$ K is orthorhombic, with the space group *Pnam*. An improper ferroelectric phase below $T_C \approx 177$ K is characterized by the space group $Pn2_1a$ and a spontaneous polarization arising along the principal axis *y*. Perhaps, AFB represents the only Be-containing material revealing an incommensurate phase between the phase transition (PT) points T_C and T_i [1].

Some data on the basic optical properties of AFB can be found in the literature. In particular, the dispersion of refractive indices in the visible optical range has been tabulated and well described by a standard Sellmeier formula (see Refs. [5, 6]). However, the temperature behaviour of the refractive indices of AFB, which is of primary importance at least for the knowledge of temperature stability of this ferroic crystal, is much less known. While the study [7] forecasts the inequality $n_x < n_z < n_y$, which contradicts the dispersion data [5], the only work [6] where the temperature dependences of the refractive indices have been reported states a very different situation, $n_y < n_x < n_z$, for most of the temperatures in

the interval 80–400 K. In other words, even fundamental information on the optical sign of AFB and a correspondence of the refractive indices n_g, n_m and n_p to the principal crystallographic axes is not reliable.

As a matter of fact, there are some problems even with the results [6]. First, it is well known that, contrary to the dielectric permittivity measured along the polar axis in AFB which behaves anomalously at the PT point T_C (see, e.g., Refs. [8, 9]), the optical birefringence changes just at the paraelectric–incommensurate PT T_i [7, 8, 10]. Then it would be very suspicious if the refractive indices behaved quite differently. Nevertheless, according to the data [6], the birefringence dependence $n_x(T)$ changes its slope at T_i, while $n_y(T)$ and $n_z(T)$ have anomalies at T_C. Second, the PT temperatures detected in Ref. [6] are essentially higher that those reported in a bulk of literature (see the T_C and T_i values cited above).

It is also known that the birefringence dispersion for the AFB crystals in the visible range can have a nonmonotonic character, which is a consequence of a so-called 'isotropic' (or 'zero-birefringence') point λ_0 and can be explained by a (T_0, λ_0)-diagram of a quasi-isotropic state [11]. This effect implies a number of applications [12–16]. Even irrespective of availability of the quasi-isotropic point in a given crystal, any possibility for a tuning of its birefringence (e.g., a temperature-driven tuning) would be promising for development of the light filters built on engineered birefringence [17–19].

The influence of temperature on the birefringence in AFB, which is also important from the viewpoint of PT investigations, has been reported in a number of studies [7, 8, 10, 20, 21]. They have been performed only in a narrow vicinity of the PTs, using Berek compensating [7], modified Senarmont [21], combined Senarmont and compensating [8] and HAUP [10] methods. Like in case of the refractive indices, strong discrepancies can be found among these results. For instance, the data [7, 8, 21] for *y*-cut AFB agree with each other only qualitatively but not quantitatively, while the results [8] derived for the *x*- and *z*-cuts at the laser wavelength 632.8 nm in many details contradict those reported in Ref. [7]. This refers to the absolute values and signs, the temperature increase or decrease, the values and the signs of the slope changes occurring at T_i, the exact PT temperatures, the availability of peculiarities at T_C, etc. Note that no information on the working wavelength has been provided in the work [7], while the data [10] obtained at 632.8 nm refers to a non-direct crystal cut [101]. As a result of our analysis, one can conclude that the information available in the literature on the temperature behaviour of the optical birefringence and the appropriate effect of the PTs in AFB is far from completeness.

The aim of the present work is to study the refractive indices and the optical birefringence of the AFB crystals in a wide temperature range and elucidate the availability of quasi-isotropic states and the influence of the PTs on the fundamental optical characteristics.

2. Experimental

2.1. General

We grew the AFB single crystals with a canonical method of slow evaporation at the room temperature, using high-grade initial substances. Our crystals had a shape of cut-off pyramids with strongly developed verges and typical dimensions 10×5×5 mm^3. Their high optical quality was proved both visually and under optical polarization microscope. Crystal

samples of the direct *x*-, *y*- and *z*-cuts were fabricated for our optical measurements, using standard methods of sample preparation. The samples for the refractive-index measurements were 0.1÷0.2 mm thick. The samples prepared for the birefringence studies had the typical thicknesses 1÷5 mm, depending on the crystal cut and the birefringence value along a given propagation direction. We took especial care of a satisfactory plane-parallelism of the sample surfaces (see Subsection 2.2). It was estimated as $\sim 10^{-4}$ rad, using visual observations of a spatial divergence of the laser beams reflected by the surfaces.

The principal refractive indices n_x, n_y and n_z of AFB were measured in the temperature interval 77÷390 K, using an immersion method. A nitrogen cryostat and a temperature-control apparatus of an UTREKS type were employed. The accuracy of the temperature stabilization was approximately equal to 0.1 K. The optical birefringences as functions of temperature were studied at 6÷460 K in order to probe a presence of the quasi-isotropic points in the widest possible range. This was done with a spectral photometric method, using a helium cryostat and the same controlling apparatus. In case of a Senarmont technique employed in a much narrower interval of the PT points (167÷197 K), the temperature of crystal samples was changed in a quasi-continuous cooling regime, with the temperature-change rate of 0.1 K/min and a higher temperature tolerance, ~ 0.03 K.

2.2. Optical methods

The refractive indices n_i ($i = x, y, z$, with $x = a$, $y = b$ and $z = c$, and a, b and c denoting the crystallographic axes of the AFB crystals) were measured using a standard Obreimov's immersion method, with a mixture of α-monobromnaphthalene and refined petroleum being an immersion liquid. This technique has been described elsewhere (see Refs. [14, 22]). Since the experiments required a linear polarization of the light incident on a crystal sample, we used commercial Glan prisms. Our setup involved an IRF-23 refractometer equipped with an Obreimov attachment. The experiments were performed at one of standard light wavelengths in the visible range, $\lambda = 500$ nm, which was achieved with a monochromator ZMR-3. A DKSSh-1000 xenon lamp was used as a light source. The total refractive-index accuracy or the method and our apparatus amounted to $\sim (2 \div 5) \times 10^{-4}$. Due to worse temperature stabilization, the largest errors were typical for the lowest temperatures.

We measured the birefringences Δn_i ($i = x, y, z$) along the principal axes x, y and z of the Fresnel ellipsoid of the FBA crystals, using a standard spectral photometric method and an optical-polarization system polarizer–sample–analyzer with a diagonal orientation of a crystal sample. The equipment included a spectrograph DFS-8 (see Ref. [14]). Its high spectral resolution (~ 1.0 nm) enabled us to perform the interference experiments at the wavelengths 300 and 500 nm. With the temperature tolerance of our setup, the resulting errors for the optical birefringence were somewhat less than 5×10^{-5}.

For more precise and detailed studies of the birefringence in the temperature region of the PTs, a Senarmont technique was applied at the He–Ne laser wavelength $\lambda = 632.8$ nm. The appropriate setup involved a polarizer–sample–compensator–analyzer system, where a high-quality quarter-wave plate served as a compensator. The fundamentals of our universal null-polarimetric method, its practical realization in the Senarmont geometry and the possible sources of experimental errors have been described in detail in our earlier work [23]. Note that, instead of the true birefringence values Δn_i, the Senarmont method deals with the birefringence increments $\delta(\Delta n_i)$ defined according to the relation

$\Delta n_i = \delta(\Delta n_i)$ + const. The sensitivity of our Senarmont equipment amounted to 10^{-6}, whereas the resulting accuracy was notably lower, $2\cdot10^{-5}$. In case of the AFB crystals, the main limiting factor was chaotic optical-retardation changes arising due to a temperature gradient in a sample. These changes were associated with the temperature tolerance and the thermal coefficient $\mathrm{d}(\Delta n_i)/\mathrm{d}T$. Another optical-retardation changes occurring through the light-beam cross-section appeared due to a deviation of sample surfaces from an ideal plane-parallelism. On the other hand, the imperfections of polarizers and optical windows of the cryostat and the effect of multiple light reflections contributed much less into the experimental errors (see also the analysis [23]).

3. Results and discussion

3.1. Refractive indices

Fig. 1 shows the temperature dependences of the refractive indices of AFB in the region 77÷390 K. One can see that the inequality $n_y < n_x < n_z$ holds true at most of the temperatures in the region under test. This fact and the refractive-index values obtained by us agree satisfactorily with the earlier dispersion [5] and temperature [6] results but contradict the prediction $n_x < n_z < n_y$ [7]. The refractive indices of the optically biaxial AFB crystals at the room temperature (T = 293 K) are equal to $n_g = n_x = 1.4038$, $n_m = n_z = 1.4034$ and $n_p = n_y = 1.3973$. The refractive index n_x acquires its highest maximum, $n_x = 1.4085$, near the PT point T_i, whereas the other indices at this temperature amount to $n_y = 1.3980$ and $n_z = 1.4064$. For a comparison, the study [6] predicts a rather different result, the inequality $n_z > n_x$ at T_i. Notice also that the refractive indices n_x and n_z are close to each other, thus indicating that the birefringence Δn_y should be small enough (see below).

According to the work [7], only one of the refractive indices of AFB has to reveal notable temperature changes, with the other two indices being weakly dependent on temperature. However, Fig. 1 demonstrates that the former statement refers to the two indices n_x and n_z, whereas only the temperature dependence $n_y(T)$ is gently sloping. As seen from Fig. 1, the only anomaly observed in the $n_i(T)$ dependences roughly corresponds to the normal–incommensurate PT and occurs at ~ 182÷184 K. Therefore one can reject the hypothesis [6] that different components of the optical susceptibilities can have anomalies at either T_i or T_C (see also the optical birefringence data below). Moreover, we cannot detect any trace of the PTs above 200 K (cf. with Ref. [6]).

Sometimes it is stated in the literature (see, e.g., Ref. [6]) that the optical parameters should reveal linear (or almost linear) temperature changes inside the normal phase. Fig. 1 testifies that this can be true only in relatively narrow temperature intervals while, in general, the temperature nonlinearities in the refractive indices cannot be ignored. This is confirmed the best by the $n_y(T)$ behaviour. In spite of nonlinear temperature dependences of the refractive indices above T_i, the approximate thermal coefficients $\mathrm{d}n_i/\mathrm{d}T$ can still be of some use (e.g., in order to estimate temperature stability). We have $\mathrm{d}n_x/\mathrm{d}T \approx -5.1\times10^{-5}$ K^{-1}, $\mathrm{d}n_y/\mathrm{d}T \approx -1.8\times10^{-5}$ K^{-1} and $\mathrm{d}n_z/\mathrm{d}T \approx -3.6\times10^{-5}$ K^{-1}. Note that these results are in contrast with the result $|\mathrm{d}n_z/\mathrm{d}T| > |\mathrm{d}n_x/\mathrm{d}T|$ [6].

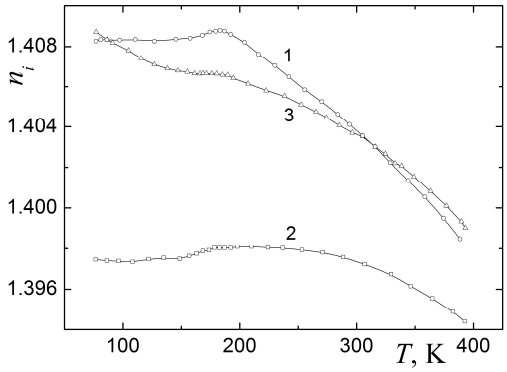

Fig. 1. Temperature dependences of refractive indices n_x (circles, curve 1), n_y (squares, curve 2) and n_z (triangles, curve 3) of the AFB crystals.

Fig. 1 demonstrates a general temperature trend, a steady approach of different refractive indices to each other at the highest temperatures. This leaves room for speculations about the existence of a hypothetic higher-symmetry (e.g., hexagonal) praphase, which really occurs in some of the A_2BX_4-family crystals.

Finally, Fig. 1 evidences that the temperature curves $n_x(T)$ and $n_z(T)$ become crossed twice, with the appropriate quasi-isotropic points $T_{01} \approx 87$ K ($n_{x,z} = 1.4083$) and $T_{02} \approx 312$ K ($n_{x,z} = 1.4032$), which correspond to the quasi-isotropic wavelength $\lambda_0 = 500$ nm. The FBA crystals become optically uniaxial at the points (T_{0i}, λ_0), with the principal direction y being the optic axis. However, such a method of finding the quasi-isotropic points is not accurate enough due to a relatively low refractive-index accuracy and a small angle of crossing of the curves $n_x(T)$ and $n_z(T)$. The more refined positions of the quasi-isotropic points in the AFB crystals will be determined on the basis of direct and more reliable birefringence data.

3.2. Optical birefringence and isotropic points

The wide-range temperature dependences of the optical birefringences Δn_i in AFB are displayed in Fig. 2. They refer to the two light wavelengths, 300 and 500 nm. As seen from Fig. 2, Δn_x and Δn_z are large and, respectively, positive and negative, whereas Δn_y is notably smaller and changes its sign twice. Note that a self-consistent definition of the birefringences should imply the condition

$$\sum_i \Delta n_i = 0 \,. \tag{1}$$

As a result, we arrive, e.g., at the following definitions:

$$\Delta n_x = n_z - n_y \,,\ \Delta n_y = n_x - n_z \,,\ \Delta n_z = n_y - n_x \,. \tag{2}$$

Eq. (1) can be used as a criterion of reliable and correct birefringence measurements. We exemplify a successful verification, with the criterion (1), of our experimental data obtained at 300 nm (see the insert in panel (a) of Fig. 2).

On the other hand, all of the birefringences found in the study [7], including Δn_z, are positive, which is not consistent with Eq. (1). The analysis of the results [7] testifies that the erroneous conclusions of this work on the refractive indices (see above) can be caused by the inconsistent working definition $\Delta n_x = n_y - n_z$, which is adopted in Ref. [7] together with the last two formulae in Eq. (2). By the way, all the Δn_i values measured in the study [8] (in particular, the birefringence Δn_z) are also positive. However, after considering properly the

difference in the Δn_z signs, the results [8] become consistent with our results in both the absolute values (the differences being less than 5%) and the main temperature trends. Nonetheless, the spontaneous change in the $\Delta n_z(T)$ dependence occurring below the PT points [7] remains quite different from our data, even if we take into account the difference in the Δn_z signs mentioned above. We suppose that some extra errors must be present in the results $\Delta n_z(T)$ [7].

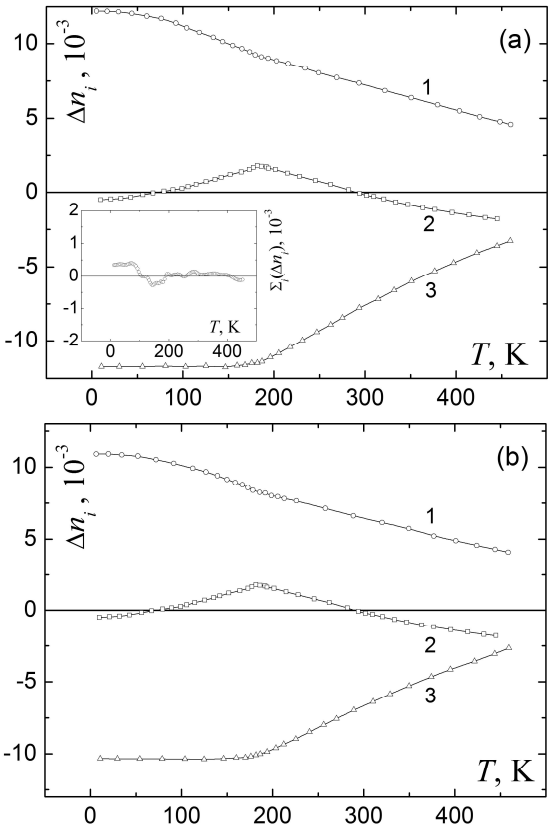

Fig. 2. Temperature dependences of birefringences Δn_x (circles, curves 1), Δn_y (squares, curves 2) and Δn_z (triangles, curves 3) of the AFB crystals, as obtained at 300 nm (panel a) and 500 nm (panel b). The insert in panel (a) shows a sum of all birefringences Δn_i, which must be zero according to definition (see the text and Eq. (1)).

Good enough compliance of our results with those of Ref. [8] implies that the optical dispersion in the visible range or, at least, in the region 500÷633 is relatively weak. Another proof of this conclusion is the difference less than 13% between all of our birefringences measured at 300 and 500 nm. Moreover, the corresponding $\Delta n_y(T)$ dependences in Fig. 2a and Fig. 2b are practically the same. We would like to stress that a practical absence of the birefringence dispersion for the propagation direction [010] is not a quite new result. This situation is typical for a number of A_2BX_4 crystals in the vicinity of their quasi-isotropic points where the dispersion can have normal, anomalous or nonmonotonic character, or can be simply zero (see, e.g., Ref. [11]).

Detailed enough data obtained for the optical birefringence enables one to find the quasi-isotropic points in the AFB crystals. We have two such points for the light propagating along the y axis: $T_{01} \approx 71.2$ K and $T_{01} \approx 290.4$ K at 300 nm, and $T_{01} \approx 71.4$ K and $T_{01} \approx 290.4$ K

at 500 nm. Notice that the temperature difference of these points found at different optical wavelengths is less than 0.2 K, which is close to the temperature tolerance. This agrees perfectly with an almost vertical curves of the quasi-isotropic states in the coordinates (T_0, λ_0) [11]. In other words, the quasi-isotropic states occur approximately at the same temperatures T_{0i}, irrespective of the wavelength. There is another point of interest to our T_{0i} data. It has been demonstrated [11] that the coordinates (T_0, λ_0) depend on the structural defects present in crystal samples (as-grown, annealed or aged, or X-ray irradiated crystals) so that a more perfect and defect-free structure reveals lower temperatures T_{0i} [11]. Since our T_{0i} values are notably lower than the maximal values ~ 77 K and ~ 310 K found in Ref. [11], we have an indirect proof of a high quality of our single crystals. Finally, a nearly linear $\Delta n_y(T)$ function in the vicinity of the isotropic points T_{0i} in the AFB crystals can be promising for optical thermometry.

Now we turn out attention to the general characteristics of the temperature behaviour of our birefringences. Although the studies [7, 8, 10, 21] state a linear character of the $\Delta n_y(T)$ dependences inside the normal phase, this is a consequence of narrower temperature regions examined in the above works. In fact, we observe in Fig. 2 some nonlinearities, although the introduction of (linear) thermal coefficients $\frac{\mathrm{d}(\Delta n_i)}{\mathrm{d}T}$ seems to be reasonable. They are given by $\frac{\mathrm{d}(\Delta n_x)}{\mathrm{d}T} \approx -1.5\times10^{-5}\ \mathrm{K}^{-1}$, $\frac{\mathrm{d}(\Delta n_y)}{\mathrm{d}T} \approx -1.4\times10^{-5}\ \mathrm{K}^{-1}$ and $\frac{\mathrm{d}(\Delta n_z)}{\mathrm{d}T} \approx 2.7\times10^{-5}\ \mathrm{K}^{-1}$ at the wavelength 500 nm. Note that the order of magnitude of these parameters is the same as that of the linear thermal coefficients of the refractive indices.

3.3. Influence of PTs

Let us proceed to the influence of PTs in AFB on its optical characteristics. Fig. 3 shows the $\delta(\Delta n_i)(T)$ dependences obtained at the wavelength 632.8 nm with the Senarmont method in a closer region of the PTs. It is seen from Fig. 3 that only the normal–incommensurate PT at T_i affects the birefringence and causes 'kinks' in the $\delta(\Delta n_i)(T)$ dependences. This fact complies with the earlier experimental data [7, 8].

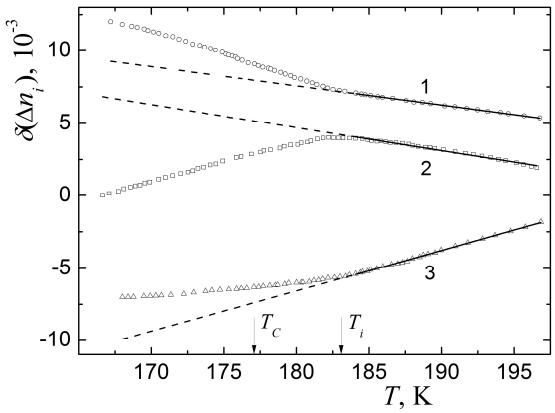

Fig. 3. Temperature dependences of birefringence increments $\delta(\Delta n_x)$ (circles, curve 1), $\delta(\Delta n_y)$ (squares, curve 2) and $\delta(\Delta n_z)$ (triangles, curve 3) of the AFB crystals, as obtained in the region of PTs at 632.8 nm. For convenience of visualization, the first data points measured at the lowest temperatures are put to be $\delta(\Delta n_x) = 12\times10^{-3}$, $\delta(\Delta n_y) = 0$ and $\delta(\Delta n_z) = -7\times10^{-3}$. Dashed lines are linear fits inside the normal phase and vertical arrows indicate the PT points.

In order to find the PT points with a high accuracy, we use the approach based upon the temperature derivatives $\zeta(T) = \frac{\mathrm{d}}{\mathrm{d}T}\delta(\Delta n)(T)$ of the birefringences [24]. Let us explain this approach in brief. According to the crystal symmetry, the equilibrium spontaneous changes Δn^S of the birefringence should be associated with the macroscopically averaged order parameter η of the normal–incommensurate PT, i.e. we have $\Delta n^S \sim \langle \eta^2 \rangle$. The total birefringence and its spontaneous part are linked by the relation $\Delta n^S(T) = \Delta n(T) - \Delta n^B(T)$, with the background term usually approximated by a linear function of temperature ($\Delta n^B(T) = B_0 + B_1 T$), and $\Delta n(T) = \delta(\Delta n)(T)$ + const (see Subsection 2.2). Then one obtains [25]

$$\begin{aligned} \zeta(T) &\equiv \tfrac{\mathrm{d}}{\mathrm{d}T}\delta(\Delta n)(T) = \tfrac{\mathrm{d}}{\mathrm{d}T}\Delta n(T) \\ &= \tfrac{\mathrm{d}}{\mathrm{d}T}(\Delta n^S(T) + \Delta n^B(T)) \sim \tfrac{\mathrm{d}}{\mathrm{d}T}\langle \eta^2(T) \rangle + \zeta_B \end{aligned}, \tag{3}$$

with $\zeta_B = B_1$ denoting a constant background term.

Now a suitable theoretical model for the $\langle \eta^2(T) \rangle$ function should be adopted. It is known that, in the region of relatively weak fluctuations around the PT, this function can be well described by a first fluctuation correction to the Landau theory [25] (see also the review [26]). After consideration of Eq. (3), this gives the following phenomenological relations which are best expressed in terms of the reduced temperature $\tau = (T - T_i)/T_i$:

$$\begin{aligned} \zeta(\tau) &= \zeta_B + \zeta_L + \lambda_- |\tau|^{-1/2} \quad (\tau < 0), \\ \zeta(\tau) &= \zeta_B + \lambda_+ \tau^{-1/2} \quad (\tau > 0). \end{aligned} \tag{4}$$

Here ζ_B is independent of the PT although, in general, its dependence on temperature cannot be excluded, ζ_L denotes a constant 'Landau jump' of $\zeta(\tau)$, which arises in a zero approximation of the mean-field theory, and $\lambda_\pm$ are constants. Note that the relation $\lambda_- / \lambda_+ = \sqrt{2}$ takes place for the amplitudes λ_+ and λ_- in case of the XY-system, which represents a canonical theoretical model for the normal–incommensurate PTs.

One can see from Eqs. (4) that the $\zeta(T)$ function manifests a sharp peak at the PT point T_i, which can be used for finding this point with the highest possible accuracy enabled by the experimental errors. Moreover, the alternative approach (i.e., finding of the PT temperature as a point where the Δn_i function has a 'kink') is, simply speaking, incorrect [26, 27]. The examples of smoothed temperature dependences $\zeta_i(\tau)$ calculated from the $\delta(\Delta n_x)$ and $\delta(\Delta n_z)$ birefringences are shown in Fig. 4. One can obtain $T_i \approx 183.1$ K as an average temperature position of the $\zeta_i(T)$ peaks. Since the incommensurate–ferroelectric PT point T_C can hardly be determined with the temperature dependences of our optical characteristics, we take the value $T_C \approx 177$ K found earlier for our crystal samples [9]. Note that, besides of the anomaly at T_i, the authors [21] have found a weak extra peculiarity in the $\delta(\Delta n_y)$ dependence at T_C. However, we cannot consider it as a reliable experimental fact in our $\zeta_i(T)$ functions.

Now one can find the limits of the temperature region around the PT where the first fluctuation correction to the Landau theory and the Landau model itself are applicable. It is given by a modified Ginzburg criterion [25]:

$$G << |\tau| << 1 \ \ (\text{or } G << |\tau| << G^{1/3}), \tag{5}$$

which is expressed in terms of the Ginzburg number G. One can determine the G parameter in the manner offered in the work [25]. First, one can approximately calculate the ζ_L parameter involved in Eqs. (4) as a difference between the 'settled' derivative values in the incommensurate and normal phases. Then the Ginzburg number G can be found as a τ value at which the deviation from the plain Landau theory (i.e., the term $\lambda_{\pm}|\tau|^{-1/2}$) is equal to ζ_L. Using the incommensurate- and paraelectric-phase data of Fig. 4 for both the $\zeta_x(\tau)$ and $\zeta_z(\tau)$ dependences, we arrive at the average value $G \approx 2.5\times10^{-3}$ which corresponds to the relative-temperature region $|T - T_i| \approx 0.5$ K around the PT point. Eventually, such a small Ginzburg parameter seems to be natural because the peaks of the $\zeta_i(\tau)$ functions are very sharp (see Fig. 4). According to the first inequality in Eqs. (5), we estimate the applicability limits as, e.g., $0.02 < |\tau| < 0.1$. This yields the temperature interval 3.7 K < (T_i – T) < 18 K below the PT point T_i. Since we have $G^{1/3} \approx 0.14$, the second formula in Eqs. (5) gives a similar estimation.

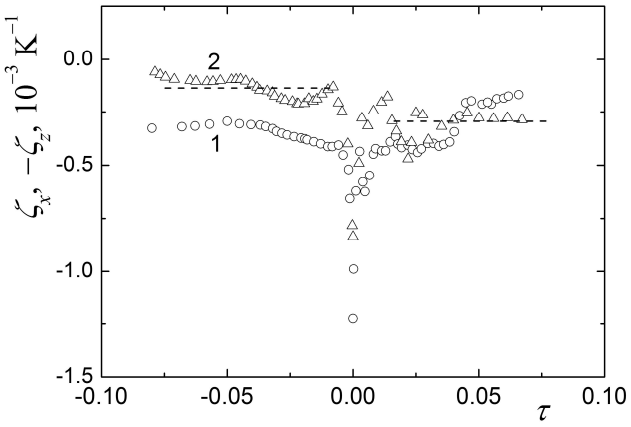

Fig. 4. Smoothed dependences of temperature derivatives ζ_x (circles, 1) and ζ_z (triangles, 2) of the birefringences in AFB on the reduced temperature $\tau = (T - T_i)/T_i$, as obtained from the data of Fig. 3. Dashed lines indicate approximate average levels $\zeta_B + \zeta_L$ and ζ_B of the derivative ζ_z in the low-temperature (left) and normal (right) phases, respectively (see Eqs. (4) and the appropriate explanations).

The G value obtained for our AFB crystals deserves a separate discussion. First, a comparison with different crystals of the A_2BX_4 family seems to be relevant. We have $G \approx 3\cdot10^{-3}$ for Cs_2CdBr_4 and $G \approx 2\cdot10^{-3}$ for Cs_2HgBr_4 [27], $G \approx 5\times10^{-3}$ for K_2SO_4, $G \approx 3\times10^{-2}$ for Rb_2SO_4 and $G \approx 7\times10^{-3}$ for Rb_2ZnCl_4 [26]. In other words, our Ginzburg number is slightly lower though the same in the order of magnitude. Second, a worthwhile fact is that the crystals with imperfections and structural defects typically reveal larger G values. For instance, we have $G \approx (2\div3)\times10^{-3}$ and $G \approx 7\times10^{-3}$ respectively for high-quality and imperfect $[N(CH_3)_4]_2ZnCl_4$ crystals [27]. The Ginzburg numbers for stoichiometric and nonstoichiometric $Pb_5Ge_3O_{11}$ crystals are also significantly different: respectively $G \approx (5\div10)\times10^{-3}$ [24, 26] and $G \approx 2.5\times10^{-2}$ [26]. This phenomenon has been explained [27] as follows: the experimental G parameter involves the intrinsic (due to the order-parameter fluctuations) and extrinsic (due to the structural defects) contributions, i.e. the defects cause

an extra broadening of the critical anomalies in the vicinity of the PT temperatures [28] (see also Eqs. (3)). Then a very small G parameter peculiar for our FBA crystals should indirectly imply a low concentration of their defects and so a relatively high crystal perfection (see also the discussion [9]).

Now that we know the applicability limits for the mean-field theory, a phenomenological analysis of our birefringence data becomes possible. The spontaneous birefringence increments $\Delta n^S(T)$ can be found by extracting the linear background terms $\Delta n^B(T)$ (see the dash lines in Fig. 3) from the $\delta(\Delta n_i)(T)$ dependences. Fig. 5 displays the resulting $\Delta n_i^S(T)$ curves on the double logarithmic scale. One can get convinced that the experimental data are well fitted by straight lines in the region 3 K < (T_i – T) < 16 K which correlates well with the theoretical estimation. The slopes of those lines for the Δn_x^S, Δn_y^S and Δn_z^S increments are respectively equal to 1.00, 1.05 and 1.02.

Following from the above experimental data, let us characterize the incommensurate PT. We remind of the standard relations $\Delta n^S \sim \langle \eta^2 \rangle$ and $\langle \eta^2(T) \rangle \sim (T_i - T)^{2\beta}$, where β is the critical index of the order parameter. Then the spontaneous birefringence data allows us to find the β value from the formula

$$\Delta n^S \sim (T_i - T)^{2\beta} . \qquad (6)$$

It is known that the XY-model predicts the value $\beta = 0.35$ in the critical temperature region. Quite naturally, this value does not conform to our experimental results. On the other hand, the behaviour of the equilibrium order parameter η_0 outside the critical region is given by a simple Landau formula $\langle \eta^2 \rangle \sim \eta_0^2 \sim (T_i - T)^{2\beta} = (T_i - T)$, with β = ½. This classical value agrees perfectly with our experiments, from which the average exponent $2\beta \approx 1.02 \pm 0.03$ follows. It is interesting that the studies of spontaneous gyration in $Pb_5Ge_3O_{11}$-family crystals with a proper ferroelectric PT, which have been carried out according to the same technique, have revealed non-classic critical indices $\beta \approx 0.30 \div 0.40$ [24, 29]. In particular, the value $\beta \approx 0.40 \pm 0.01$ has been derived for pure $Pb_5Ge_3O_{11}$ [29], unlike to what is observed for the AFB crystals.

Finally, we have attempted to interpret the spontaneous changes of the refractive indices, in spite of much poorer experimental data available in the region of the PTs (typically from 4 to 5 data points lying in the temperature limits given by the Ginzburg criterion – see Fig. 1). We do not present the appropriate log–log plots which yield in the critical exponent roughly equal to $2\beta \sim 0.8 \div 1.0$. Therefore, our refractive-index results do not contradict the main conclusions on the PTs drawn from the birefringence data.

Summing up, the temperature behaviour of the optical birefringence in AFB is governed solely by the normal–incommensurate PT at T_i, which is successfully described by the canonical mean-field theory. In this respect we stress again that no influence of the improper ferroelectric PT at T_C can be observed in the optical properties of AFB. The physical reasons for such a difference from the behaviour of the dielectric properties of the AFB crystals (see Ref. [9]) still have to be clarified. Finally, we note that there have been some attempts to interpret the spontaneous changes $\Delta n^S(T)$ in the AFB crystals in terms of their spontaneous polarization $P_S(T)$ arising as a secondary effect in the improper ferroelectric phase. The first

attempt [20] does not seem to be convincing, since (i) the dependence Δn^S on P_S^2 is notably nonlinear and, moreover, it does not pass through the origin point $(0, 0)$; (ii) this interpretation does not agree with the subsequent experimental facts reported by the same author [8]. The other attempt has been due to the work [21] where $\Delta n_y(T)$ is associated with both the incommensurate order parameter η and the spontaneous polarization P_S. However, the appropriate experimental data (see Fig. 2 in Ref. [21]) is so scarce that it is difficult to determine the very PT points, to say nothing of the spontaneous increments Δn^S.

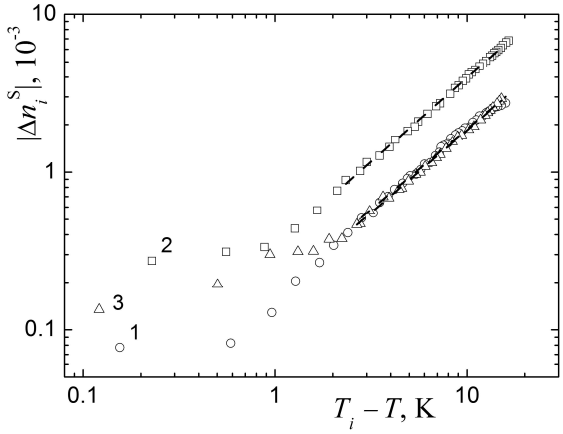

Fig. 5. Log–log dependences of the absolute values of spontaneous birefringences Δn_x^S (circles, 1), Δn_y^S (squares, 2) and Δn_z^S (triangles, 3) for the AFB crystals on the relative temperature ($T_i - T$), as obtained from the data of Fig. 3. Dashed lines indicate linear fittings according to Eq. (6) in the temperature region where the mean-field phenomenology can be applied (see the text).

4. Conclusions

In the present work we have studied the fundamental optical susceptibilities associated with the refractive indices of the AFB crystals in the range 77÷390 K. The anisotropy of the optical susceptibilities associated with the birefringence has been measured at the two wavelengths, 300 and 500 nm, in a wider temperature interval ranging from the liquid-helium temperatures to 460 K. The main characteristics of the optical indicatrix of biaxial AFB depending on the temperature have been examined. In particular, it has been shown that the relation $n_y < n_x < n_z$ takes place at most of the temperatures under test. We have demonstrated that the discrepancies found in the earlier optical studies of FBA can be related to inconsistent definitions of the birefringences measured along different principal Fresnel-ellipsoid axes. The approximate values of thermal coefficients of the refractive indices and the birefringences have been found for the high-temperature normal phase.

We have testified indirectly that the optical dispersion in the AFB crystals should be weak enough, which is especially true of the principal propagation direction *y*. We have also found the two quasi-isotropic points in the AFB crystals: $T_{01} \approx 71.2$ K and $T_{01} \approx 290.4$ K at 300 nm, and $T_{01} \approx 71.4$ K and $T_{01} \approx 290.4$ K at 500 nm. The birefringence Δn_y goes through zero at these points and the crystal becomes optically uniaxial, with the optic axis being parallel to the *y* axis. It is important that the temperature positions T_{0i} of the isotropic points are almost independent of the light wavelength, i.e. the quasi-isotropic states occur approximately at the same temperatures T_{0i}, irrespective of the wavelength.

Some characteristics of the PTs taking place in the ferroelectric, incommensurately modulated AFB crystals have been revealed through the studies of their optical properties. In particular, we have demonstrated that, unlike the dielectric permittivity, the optical characteristics of AFB are affected only by the normal–incommensurate PT. The attempts to associate, at least partly, the temperature behaviour of the refractive indices and the birefringence with the improper ferroelectric PT located at T_C have proved to be unsuccessful. The approach of temperature derivatives has been employed to detect the PT $T_i \approx 183.1$ K with high accuracy.

The same approach has been used for finding the temperature region around T_i where the critical fluctuations in FBA are small and the canonical mean-field phenomenology works well. This region is determined by the Ginzburg criterion, with a very small Ginzburg number ($G \approx 2.5 \times 10^{-3}$). A comparison of our G with the corresponding parameters known for some other crystals, mostly those belonging to the A_2BX_4 family, along with relatively low isotropic-point temperatures T_{0i}, confirm indirectly a high quality and low defect concentration in our FBA single crystals. Finally, the spontaneous birefringence increments arising due to the incommensurate PT outside the critical region of AFB have been successfully described by the canonical mean-field theory, with the critical index of the order parameter $\beta \approx 0.50$.

References

1. Cummins, H. Z. (1990). Experimental studies of structurally incommensurate crystal phases. *Phys. Rep.*, *185*(5-6), 211-409.
2. Strukov, B. A., Levanyuk, A. P. (1998). *Ferroelectric Phenomena in Crystals: Physical Foundations*.
3. Palatinus, L., & Smaalen, S. (2004). The ferroelectric phase transition and modulated valence electrons in the incommensurate phase of ammonium tetrafluoroberyllate. *Ferroelectrics*, *305*(1), 49-52.
4. Brik, M. G., & Kityk, I. V. (2007). Spectroscopic and crystal field studies of $(NH_4)_2BeF_4:Co^{2+}$. *Solid State Commun.*, *143*(6-7), 326-330.
5. Rudysh, M. Y., Fedorchuk, A. O., Stadnyk, V. Y., Shchepanskyi, P. A., Brezvin, R. S., Horon, B. I., ... & Gorina, O. M. (2023). Structure, electronic, optical and elastic properties of $(NH_4)_2BeF_4$ crystal in paraelectric phase. *Current Appl. Phys.*, *45*, 76-85.
6. Romanyuk, M. O. (2006). Spectral refractometry of the ferroics of triglycine sulfate group, rochelle salt and potassium sulfate crystals. *J. Phys. Stud., 10*(4)*,* 358–380.
7. Strukov B A, (1961). Temperature dependence of birefringence in ammonium sulfate and fluoroberyllate crystals. *Kristallografiya*. *6,* 635–639
8. Anistratov, A. T., & Melnikov. S. V. (1973). Thermooptical and dielectric properties of $(HN_4)_2BeF_4$ in vicinity of ferroelectric transition. *Kristallografiya*, *18*(6), 1289-1291.
9. Horon, B. I., Kushnir, O. S., Shchepanskyi, P. A., & Stadnyk, V. Y. (2023). Temperature dependence of dielectric permittivity in incommensurately modulated phase of ammonium fluoroberyllate. *Condens. Matter Phys.,* 2*5,* 43704.
10. Kobayashi, J., Uesu, Y., Ogawa, J., & Nishihara, Y. (1985). Optical and x-ray studies on incommensurate phase transitions of ferroelectric ammonium fluoroberyllate $(NH_4)_2BeF_4$. *Phys. Rev. B.*, *31*(7), 4569.
11. Romanyuk, M. O., & Stadnyk, V. Y. (1997). The action of mechanical stress and other influences on birefringence inversion of $LiKSO_4$ and $(NH_4)_2BeF_4$ crystals. *Ferroelectrics*, *192*(1), 235-241.
12. Kushnir, O. S., Dzendzelyuk, O. S., Hrabovskyy, V. A., & Vlokh, O. G. (2004). Optical transmittance of dichroic crystals with “isotropic point”. *Ukr. J. Phys. Opt., 5*(1), 1-5.
13. Glazer, A. M., Zhang, N., Bartasyte, A., Keeble, D. S., Huband, S., Thomas, P. A., ... & Hlinka, J. (2012). $LiTaO_3$ crystals with near-zero birefringence. *J. Appl. Cryst.*, *45*(5), 1030-1037.
14. Shchepanskyi, P. A., Kushnir, O. S., Stadnyk, V. Y., Fedorchuk, A. O., Rudysh, M. Y., Brezvin, R. S., ... & Krymus, A. S. (2017). Structure and optical anisotropy of $K_{1.75}(NH_4)_{0.25}SO_4$ solid solution. *Ukr. J. Phys. Opt.*, *18*(4), 187-196.
15. Tan, M., Martin, A. T., Shtukenberg, A. G., & Kahr, B. (2020). Tuning the optical isotropic point of mixed crystals of ethylenediammonium sulfate/selenate. *J. Appl. Crystallogr.*, *53*(1), 51-57.

16.Yariv, A., & Yeh, P. (1983). Optical waves in crystal propagation and control of laser radiation.
17.Chu, R. H., & Town, G. (2002). Birefringent filter synthesis by use of a digital filter design algorithm. *Appl. Opt.*, *41*(17), 3412-3418.
18.Verhoeff, A. A., Brand, R. P., & Lekkerkerker, H. N. W. (2011). Tuning the birefringence of the nematic phase in suspensions of colloidal gibbsite platelets. *Mol. Phys.*, *109*(7-10), 1363-1371.
19.Rothschild, M., Diest, K., & Liberman, V. (2017). *U.S. Patent No. 9,841,606*. Washington, DC: U.S. Patent and Trademark Office.
20.Anistratov, A. T. (1972). Optical properties of ferroelectrics. digressions from phenomenological theory. *Revue de Physique Appliquée*, *7*(2), 77-79.
21.Koňák, Č., & Matras, J. (1976). Birefringent and electrooptical properties of $(NH_4)_2BeF_4$, *Czech. J. Phys. B*, *26*(5), 577-584.
22.Stadnyk, V. I., Romanyuk, M. O., Kushnir, O. S., Brezvin, R. S., Franiv, A. V., & Gaba, V. M. (2010). Temperature and spectral changes in the refractive indices of $LiKSO_4$ crystals under uniaxial pressures. *Int. J. Mod. Phys. B*, *24*(32), 6219-6233.
23.Kushnir, O. S., Burak, Y. V., Bevz, O. A., & Polovinko, I. I. (1999). Crystal optical studies of lithium tetraborate. *J. Phys.: Condens. Matter*, *11*(42), 8313.
24.Kushnir, O. S., Shopa, R. Y., & Vlokh, R. O. (2008). Optical studies of order parameter fluctuations in solid solutions based on lead germanate crystals. *Ukr. J. Phys. Opt.*, *9*(3), 169-181.
25.Ivanov, N. R., Levanyuk, A. P., Minyukov, S. A., Kroupa, J., & Fousek, J. (1990). The critical temperature dependence of birefringence near the normal-incommensurate phase transition in Rb_2ZnBr_4. *J. Phys.: Condens. Matter*, *2*(26), 5777-5786.
26.Romanyuk, M. O., Andrievskyy, B. V., Stadnyk, V. Y., & Kushnir, O. S. (2013). Studies of ferroics in the electronic region of spectrum. *J. Phys. Stud.*, *17*(3), 3701.
27.Kushnir, O. S., Kityk, A. V., Dzyubanski, V. S., & Shopa, R. Y. (2011). Critical behaviour of optical birefringence near the normal–incommensurate phase transition in $[N(CH_3)_4]_2ZnCl_4$ crystals under the influence of hydrostatic pressure. *J. Phys.: Condens. Matter*, *23*(22), 225403.
28.Levanyuk, A. P., & Sigov, A. S. (1988). Defects and structural phase transitions.
29.Adamenko, D. I., & Vlokh, R. O. (2023). Critical exponents of the order parameter of diffuse ferroelectric phase transitions in the solid solutions based on lead germanate: studies of optical rotation. *Condens. Matter Phys.* 25, 43703.

B. I. Horon, O. S. Kushnir and V. Yo.Stadnyk. 2024. Temperature dependences of refractive indices and optical birefringence in ammonium fluoroberyllate. *Ukr. J. Phys. Opt.* 25, 01020 – 01032. doi: 10.3116/16091833/Ukr.J.Phys.Opt.2024.01020;

Анотація. *Досліджено показники заломлення та подвійне променезаломлення невласних сегнетоелектричних кристалів фторберилату амонію (ФБА) з несумірною фазою в широкому діапазоні температур. Вивчено температурні характеристики оптичної індикатриси ФБА та знайдено дві квазіізотропні точки, температурні положення T_0 яких практично не залежать від довжини світлової хвилі. На відміну від діелектричної проникності, на яку впливає фазовий перехід (ФП) з несумірної до сегнетоелектричної фази при T_C, на оптичні характеристики ФБА впливає лише ФП з нормальної до несумірної фази, розташований при $T_i \approx 183{,}1$ К. Використовуючи критерій Гінзбурга та експериментальне число Гінзбурга $G \approx 2{,}5\times10^{-3}$, визначено температурну область навколо T_i, де критичні флуктуації малі та застосовна класична теорія середнього поля. За межами критичної області спонтанне подвійне променезаломлення, яке виникає внаслідок несумірного ФП, ідеально описується теорією Ландау з критичним індексом параметра порядку $\beta \approx 0{,}50$.*

Ключові слова: *фторберилат амонію, оптично двовісні кристали, показники заломлення, подвійне променезаломлення, квазіізотропні стани, несумірні фазові переходи, критерій Гінзбурга, критичні індекси.*